

**Analysis of heat transfer and entropy generation for a thermally developing Brinkman-Brinkman forced convection problem in a rectangular duct with isoflux walls**

K. Hooman (Corresponding Author)<sup>1</sup> and A. Haji-Sheikh<sup>2</sup>

<sup>1</sup>School of Engineering, The University of Queensland, Brisbane, Australia

<sup>2</sup>Department of Mechanical and Aerospace Engineering, The University of Texas  
at Arlington, 500 W. First Street, Arlington, Texas 76019, USA

**Abstract**

Heat transfer and entropy generation analysis of the thermally developing forced convection in a porous-saturated duct of rectangular cross-section, with walls maintained at a constant and uniform heat flux, is investigated based on the Brinkman flow model. The classical Galerkin method is used to obtain the fully developed velocity distribution. To solve the thermal energy equation, with the effects of viscous dissipation being included, the Extended Weighted Residuals Method (EWRM) is applied. The local (three dimensional) temperature field is solved by utilizing the Green's function solution based on the EWRM where symbolic algebra is being used for convenience in presentation. Following the computation of the temperature field, expressions are presented for the local Nusselt number and the bulk temperature as a function of the dimensionless longitudinal coordinate, the aspect ratio, the Darcy number, the viscosity ratio, and the Brinkman number. With the velocity and temperature field being determined, the Second Law (of Thermodynamics) aspect of the problem is also investigated. Approximate closed form solutions are also presented for two limiting cases of  $MDa$  values. It is observed that decreasing the aspect ratio and  $MDa$  values increases the entropy generation rate.

**Keywords:** Extended weighted residuals method, porous media, viscous dissipation, thermal development, rectangular duct, Brinkman-Brinkman problem, entropy generation

**Nomenclature**

$A$	area, $m^2$
$\mathbf{A}$	matrix
$a_{ij}$	elements of matrix $\mathbf{A}$
$\mathbf{B}$	matrix
$B_m$	coefficients
Br	Brinkman number, $\mu_e U^2 / (q_w a)$
$b_{ij}$	elements of matrix $\mathbf{B}$
$\bar{b}$	aspect ratio, $\bar{b} = b/a$
$C$	duct contour, $m$
$c_p$	specific heat, $J/kg \cdot K$
$\mathbf{D}$	matrix
Da	Darcy number, $K/a^2$
$D_h$	hydraulic diameter $4A/C$ , $m$
$d_{mj}$	elements of matrix $\mathbf{D}$
$\mathbf{E}$	matrix with elements $e_{ij}$
$e_{ij}$	elements of matrix $\mathbf{E}$
$F$	required pumping power to enthalpy change ratio, $F = P^* / (\rho c_p \eta)$
$f_i, f_j$	basis functions
$G$	Green's function
$h$	heat transfer coefficient, $W/m^2 \cdot K$
$\bar{h}$	average heat transfer coefficient, $W/m^2 \cdot K$
$i, j$	indices
$K$	permeability, $m^2$
$k_e$	effective thermal conductivity, $W/m \cdot K$

$L$	duct length, $m$
$\hat{L}$	dimensionless duct length, $L/(aPe)$
$M$	$\mu_e/\mu$
$m, n$	indices
$N$	matrix dimension
$N^*$	dimensionless pressure drop, $N^* = P^*/(\mu U / K)$
$Ns$	dimensionless entropy generation rate, $Ns = \dot{S}_{gen}/(\dot{m} c_p)$
$Nu$	Nusselt number, $ha/k_e$
$Nu_D$	Nusselt number, $hD_h/k_e$
$Nu^*$	Nusselt number without viscous dissipation
$\mathbf{P}$	matrix having elements $p_{mi}$
$P^*$	negative of the applied pressure gradient, $Pa/m$
$Pe$	Péclet number, $\rho c_p a U / k_e$
$p$	pressure, Pa
$p_{mi}$	elements of matrix $\mathbf{P}$
$q^*$	dimensionless wall heat flux, $q^* = q_w a / (k_e T_i)$
$Re_D$	Reynolds number, $\rho U D_h / \mu_e$
$s$	entropy, $J/KgK$
$S$	volumetric heat source, $W/m^3$
$\dot{S}_{gen}$	Cross-sectional average of the entropy generation rate, $W/K$
$T$	temperature, $K$
$T_i$	temperature at $x=0$ , $K$
$U$	average velocity, $m/s$
$\bar{U}$	average value of $\bar{u}$

$u$	velocity, $m/s$
$\bar{u}$	dimensionless velocity, $\bar{u} = \mu u / (P^* a^2)$
$x$	axial coordinate, $m$
$\hat{x}$	$(x/a)/Pe$
$y, z$	coordinates, $m$
$\bar{y}, \bar{z}$	$y/a$ and $z/a$

**Greek**

$\Delta$	vector with elements $\delta_i$
$\delta_i$	elements of vector $\Delta$
$\theta$	dimensionless temperature
$\lambda_m$	eigenvalues
$\mu$	fluid viscosity, $N \cdot s/m^2$
$\mu_e$	effective viscosity, $N \cdot s/m^2$
$\xi$	dimensionless coordinate,
$\rho$	fluid density, $kg/m^3$
$\Phi$	transformed temperature, Eq. (24)
$\psi$	Eigenfunction
$\Omega$	vectors with element $\omega_i$
$\omega_i$	elements of vector $\Omega$

**Subscripts**

$b$	bulk
$i$	inlet condition
$s$	source effect
$w$	wall

## 1. Introduction

Designed porous media, which are of current practical importance, are usually associated with such high permeability and porosity that the Darcy flow model is not applicable while the Brinkman flow model can predict hydraulics through such hyperporous media as noted by Nield and Bejan [1]. Flow through pores, in a microscopic scale, is inherently irreversible and a part of the mechanical power is dissipated to heat as a result of viscous dissipation. Consequently, this effect at the pore level is accounted for in macroscopic scale by retaining a viscous dissipation term in the thermal energy equation where the term is proportional to the volume-averaged velocity square as first noted by Ene and Sanchez-Palencia [2] for cases where the Darcy flow model is valid. On the other hand, as noted above, there are numerous cases of practical importance, where non-Darcy effects are significant and one should model the pore level dissipation in terms of appropriate properties (of fluid and solid matrix). However, for such cases one is left with two alternatives for the viscous dissipation function as proposed by Nield [3] and Al-Hadhrami et al. [4]. Recently, Breugem and Rees [5] have reported a volume averaging procedure to come up with a general model for viscous dissipation that seems to be applicable for a Brinkman-Brinkman problem. The term 'Brinkman-Brinkman', proposed by Nield [6], refers to a problem involving a saturated porous medium in which the Brinkman momentum equation is used, and the thermal energy equation includes a viscous dissipation term involving a Brinkman number, which is the case here. It is also instructive to note that there are certain cases where one can neglect the effects of viscous dissipation as highlighted by Nield [6,7].

Regardless of the relative importance of the frictional heating compared to other heat transfer mechanisms in a system, there are some applications where one is willing to inspect the viscous dissipation effects. In an analysis of mantle flow, Bercovici [8] showed an example of the effects of viscous dissipation in self-lubricating systems. On the other hand, the recent work of Celata et al. [9] addresses an interesting application of viscous dissipation in measuring the fluid friction coefficient for flow in a microchannel. In another notable study, Murakami and Mikic [10] have stated that even for flow of air, which has a relatively small viscosity compared to common liquids, say water, through a microchannel one should consider the effects of viscous dissipation when it comes to seek an optimum design feature for either of laminar or turbulent flows. Moreover, when it comes to entropy generation minimization (EGM), which is a popular method of optimization, one should have a clear insight of the viscous dissipation as it emerges in the fluid friction term of entropy generation [11].

The groundbreaking work by Bejan [11] introduced the application of entropy generation due to heat and fluid flow as a powerful tool to optimize variety of configurations when analyzing engineering problems. Since entropy generation destroys the available work of a system, it makes good engineering sense to focus on entropy production due to heat transfer and fluid flow processes to understand the

associated entropy generation mechanisms. The literature on the topic is rich for flow through unobstructed circular tubes or parallel plate channels. Similar work, mostly restricted to the fully developed region, extended the analysis to ducts of arbitrary cross-section [12-13], to name a few.

On the other hand, modeling entropy generation in porous media is comparatively harder than the clear fluid case partly due to the increased number of variables present in the governing equations. Another source of debate is the different available models for viscous dissipation, that lead to different fluid friction irreversibility (FFI) terms, as noted earlier. Moreover, the complexity of the problem becomes clearer when one observes that, numerical or theoretical, solutions addressing the Second Law analysis of forced convection in porous ducts are mostly restricted to circular tubes or parallel plate channels [14-17], where the simplicity of the geometry allows analytical solution of closed form. Thus the question naturally arises as to whether analytical solutions, addressing heat transfer and entropy generation, for more complicated cross-sections are possible.

The method of weighted residuals was exploited by Haji-Sheikh and Vafai [18] in their study of thermally developing convection in ducts of various shapes. In a subsequent study, Haji-Sheikh [19] has applied a Fourier series method to investigate fully developed forced convection in a duct of rectangular cross-section. Haji-Sheikh et al. [20-24] have investigated heat transfer characteristics of the thermal entrance region for flow through porous ducts of arbitrary cross-sections. Applying the Fourier series method, Hooman and Merrikh [25] have analytically investigated heat transfer and fluid flow in a rectangular duct occupied by a hyperporous medium.

On the other hand, a quick look at [18-25] shows that none of these articles reported the Second Law analysis and the work addressing the issue is limited to those applying the Darcy flow model in ducts of arbitrary cross-sections [26-28] with the exception of [29] where the authors have reported heat transfer and entropy generation optimization in the fully developed region of a rectangular duct for three cases of **H1** boundary condition in the terminology of Shah and London [30]. This study treats the more general case of a thermally developing Brinkman-Brinkman problem in a duct of rectangular cross-section with walls held at a constant and uniform heat flux, i.e. the **H2** case [30]. To the authors' knowledge, not only is no analytical solution available for the First Law aspects of this problem but also the present assessment of entropy generation for a thermally developing Brinkman-Brinkman problem has not been reported elsewhere.

## 2. Analysis

### 2.1 Fluid flow analysis

For a passage with a constant but arbitrarily shaped cross-section the Brinkman momentum equation reads

$$\mu_e \left( \frac{\partial^2 u}{\partial y^2} + \frac{\partial^2 u}{\partial z^2} \right) - \frac{\mu}{K} u - \frac{\partial p}{\partial x} = 0. \quad (1)$$

Although an exact solution for hydrodynamically fully developed velocity solution is available, for convenience of symbolic manipulation, the classical Galerkin method is used for computation of velocity.

It begins by setting

$$u(y, z) = \sum_{j=1}^N \delta_j \eta_j(y, z). \quad (2a)$$

where

$$\eta_j = (a^2 - y^2)(b^2 - z^2) y^{2(m_j-1)} z^{2(n_j-1)} \quad (2b)$$

and  $\delta_j$  coefficients are the constants to be determined. Next, the substitution of  $u(y, z)$  from Eq. (2a) in momentum equation and following the procedure in [31] leads to

$$\mathbf{E} \cdot \mathbf{\Delta} = \mathbf{\Omega}, \quad (3a)$$

with matrix  $\mathbf{E}$  and vector  $\mathbf{\Omega}$  having elements

$$e_{ij} = \int_A [\mu_e \eta_i(\mathbf{y}, z) \nabla^2 \eta_j(\mathbf{y}, z) - \mu \eta_j / K] dA, \quad (3b)$$

and

$$\omega_i = \left( \frac{\partial p}{\partial x} \right) \int_A \eta_i(y, z) dA, \quad (3c)$$

Therefore, the unknown coefficients are members of the vector  $\mathbf{\Delta} = \{\delta_1, \delta_2, \dots, \delta_N\}$  obtainable from  $\mathbf{\Delta} = \mathbf{E}^{-1} \cdot \mathbf{\Omega}$ . Once the local velocity distribution is determined, the mean velocity can be obtained as

$$U = \frac{1}{A} \int_A u dA, \quad (4a)$$

and the normalized velocity is

$$\hat{u} = \frac{u}{U}. \quad (4b)$$

It is worth noting that  $A$  in Eq. (4a) is the cross-sectional area of the duct.

## 2.2 Heat transfer analysis

### 2.2.1 Governing Thermal Energy Equation

Under the local thermal equilibrium condition, the energy equation in its general form for hydrodynamically fully developed and incompressible flow is

$$(\rho c_p)_f u \frac{\partial T}{\partial x} = \frac{\partial}{\partial x} \left( k_e \frac{\partial T}{\partial x} \right) + \frac{\partial}{\partial y} \left( k_e \frac{\partial T}{\partial y} \right) + \frac{\partial}{\partial z} \left( k_e \frac{\partial T}{\partial z} \right) + S(x, y, z), \quad (5)$$

where  $S(x, y, z)$  includes the contribution of frictional heating and parameters  $(\rho c_p)_f$  and  $k_e$  are the fluid thermal capacity and the equivalent thermal conductivity, respectively. When the contribution of axial conduction is negligible, Eq. (5) reduces to

$$\frac{\partial}{\partial y} \left( k_e \frac{\partial T}{\partial y} \right) + \frac{\partial}{\partial z} \left( k_e \frac{\partial T}{\partial z} \right) + S(y, z; x) = (\rho c_p)_f u \frac{\partial T}{\partial x}. \quad (6)$$

The solution for Eq. (6) with a prescribed wall heat flux and in the presence of frictional heating is possible as

$$T(y, z; x) = \sum_{m=1}^N B_m \Psi_m(y, z) e^{-\lambda_m^2 x} \quad (7a)$$

where

$$\Psi_m = \sum_{j=1}^N d_{mj} f_j(y, z) \quad (7b)$$

The following set of basis functions satisfies the homogeneous boundary condition of the second kind along the walls,

$$f_j = \left( 1 + (m_j - 1)(1 - \bar{y}^2) \right) \left( 1 + (n_j - 1)(1 - \bar{z}^2 / \bar{b}^2) \right) \bar{y}^{2(m_j-1)} \bar{z}^{2(n_j-1)}, \quad (8)$$

for all combinations of  $m_j = 1, 2, \dots$  and  $n_j = 1, 2, \dots$ . The eigenvalues are  $\lambda_m^2$  and the coefficients  $d_{mj}$  are the members of eigenvectors  $\mathbf{d}_m$ ; they are obtainable from the relation

$$(\mathbf{A} + \lambda_m^2 \mathbf{B}) \cdot \mathbf{d}_m = 0, \quad (9)$$

where the elements of the matrices  $\mathbf{A}$  and  $\mathbf{B}$  are

$$a_{ij} = - \int_A k_e \nabla f_i(y, z) \cdot \nabla f_j(y, z) dA \quad (10a)$$

$$b_{ij} = \int_A \rho c_p u(y, z) f_i(y, z) f_j(y, z) dA. \quad (10b)$$



After determination of  $\lambda_m^2$  and  $d_{mj}$ , the appropriate mathematical steps in [32] provide the general solution. The eigenvectors  $\mathbf{d}_m$  will constitute the rows of a matrix  $\mathbf{D}$ . When the boundary conditions are homogeneous and the thermophysical properties are constant, the Green's function solution is

$$T(y, z; x) = \frac{1}{\rho c_p} \int_{\xi=0}^x d\xi \int_A G S(y', z'; \xi) dA' + \int_A u(y', z') G(y, z, x | y', z', 0) T(y', z'; 0) dA'. \quad (11)$$

wherein the Green's function is

$$G(y, z, x | y', z', \xi) = \sum_{m=1}^N \left[ \sum_{i=1}^N p_{mi} f_i(y', z') \right] \Psi_m(y, z) e^{-\lambda_m^2(x-\xi)}. \quad (12)$$

The parameters  $p_{mi}$  in Eq. (12) are members of the matrix  $\mathbf{P}=[(\mathbf{D}\cdot\mathbf{B})^T]^{-1}$  (see Chapter 10 of [32] for more details). In dimensionless space, the temperature solution in rectangular passages takes the following form

$$T(\bar{y}, \bar{z}; \hat{x}) = \frac{1}{\rho c_p} \int_{\xi=0}^{\hat{x}} d\xi \int_{\bar{z}=0}^{\bar{b}} \int_{\bar{y}=0}^1 G(\bar{y}, \bar{z}, \hat{x} | \bar{y}', \bar{z}', \xi) S(\bar{y}', \bar{z}') d\bar{y}' d\bar{z}' \\ + \int_{\bar{z}=0}^{\bar{b}} \int_{\bar{y}=0}^1 u(\bar{y}', \bar{z}') G(\bar{y}, \bar{z}, \hat{x} | \bar{y}', \bar{z}', 0) T(y, z; 0) d\bar{y}' d\bar{z}' \quad (13)$$

wherein the Green's function is

$$G(\bar{y}, \bar{z}, \hat{x} | \bar{y}', \bar{z}', \xi) = \sum_{m=1}^N \left[ \sum_{i=1}^N p_{mi} f_i(\bar{y}', \bar{z}') \right] \Psi_m(y, z) e^{-\lambda_m^2(\hat{x}-\xi)} \quad (14)$$

and

$$S(\bar{y}', \bar{z}') = \frac{\mu_e U^2}{k_e(T_i - T_w)} \left[ \frac{\hat{u}^2}{M Da} + \left( \frac{\partial \hat{u}}{\partial \bar{y}'} \right)^2 + \left( \frac{\partial \hat{u}}{\partial \bar{z}'} \right)^2 \right] \quad (15)$$

The next task is the computation of the temperature in the entrance region of rectangular passages with locally constant wall heat flux  $q_w$ . For the EWRM, the boundary conditions should be homogeneous. Therefore, the following temperature transformation, in the dimensionless form, is being used for insertion into the energy equation,

$$\theta(\bar{y}, \bar{z}; \hat{x}) = \frac{T(y, z; x) - T_i}{q_w a / k_e} = \Phi(\bar{y}, \bar{z}; \hat{x}) + \frac{\bar{y}^2}{2} + \frac{\bar{z}^2}{2b} \quad (16)$$

where  $q_w = k_e \partial T / \partial y|_{y=a} = k_e \partial T / \partial z|_{z=b}$  is the input heat flux. After substituting for  $T$  from this transformation in Eq. (15), the function  $\Phi(\bar{y}, \bar{z}; \hat{x})$  must satisfy the following equation

$$\frac{\partial^2 \Phi}{\partial \bar{y}^2} + \frac{\partial^2 \Phi}{\partial \bar{z}^2} + \frac{\mu_e U^2}{q_w a} \left[ \frac{\hat{u}^2}{MDa} + \left( \frac{\partial \hat{u}}{\partial \bar{y}} \right)^2 + \left( \frac{\partial \hat{u}}{\partial \bar{z}} \right)^2 \right] + \frac{\bar{b} + 1}{\bar{b}} = \left( \frac{u}{U} \right) \frac{\partial \Phi}{\partial \hat{x}} \quad (17)$$

Now, the new function  $\Phi(\bar{y}, \bar{z}; \hat{x})$  satisfies the boundary conditions  $\partial \Phi / \partial \bar{y} \big|_{\bar{y}=0} = \partial \Phi / \partial \bar{y} \big|_{\bar{y}=1} = 0$ ,  $\partial \Phi / \partial \bar{z} \big|_{\bar{z}=0} = \partial \Phi / \partial \bar{z} \big|_{\bar{z}=\bar{b}} = 0$  and the entrance condition  $\Phi(\bar{y}, \bar{z}; 0) = -(\bar{y}^2 + \bar{z}^2 / \bar{b}) / 2$ .

The equation for  $\Phi(\bar{y}, \bar{z}; \hat{x})$  contains a heat source expression that results from viscous dissipation in a porous medium modeled by the Brinkman equation, in the form recommended in [4]. Also it contains an additional source term that emerged following transformation. This suggests a development of two separate solutions; first,  $\Phi_1(\bar{y}, \bar{z}; \hat{x})$  is neglecting the contribution of viscous dissipation and using the quantity  $(\bar{b} + 1) / \bar{b}$  as the only contribution for the wall effect. The second solution  $\Phi_2(\bar{y}, \bar{z}; \hat{x})$  is to use  $S(y', z', \xi)$  in the Green's function solution for the frictional contribution and this makes  $\Phi(\bar{y}, \bar{z}; \hat{x}) = \Phi_1(\bar{y}, \bar{z}; \hat{x}) + Br \Phi_2(\bar{y}, \bar{z}; \hat{x})$  with  $Br = \mu_e U^2 / (q_w a)$ . Splitting Eq. (13) into two equations; the first contribution is

$$\begin{aligned} \Phi_1(\bar{y}, \bar{z}; \hat{x}) = & \int_{\xi=0}^{\hat{x}} d\xi \int_{\bar{z}=0}^{\bar{b}} \int_{\bar{y}=0}^1 G(\bar{y}, \bar{z}, \hat{x} | \bar{y}', \bar{z}', \xi) \left( \frac{1+\bar{b}}{\bar{b}} \right) d\bar{y}' d\bar{z}' \\ & - \int_{\bar{z}=0}^{\bar{b}} \int_{\bar{y}=0}^1 u(\bar{y}', \bar{z}') G(\bar{y}, \bar{z}, \hat{x} | \bar{y}', \bar{z}', 0) \left( \frac{\bar{y}^2}{2} + \frac{\bar{z}^2}{2\bar{b}} \right) d\bar{y}' d\bar{z}'. \end{aligned} \quad (18)$$

and the second one is

$$\Phi_2(\bar{y}, \bar{z}; \hat{x}) = \int_{\xi=0}^{\hat{x}} d\xi \int_{\bar{z}=0}^{\bar{b}} \int_{\bar{y}=0}^1 G(\bar{y}, \bar{z}, \hat{x} | \bar{y}', \bar{z}', \xi) \left[ \frac{\hat{u}^2}{MDa} + \left( \frac{\partial \hat{u}}{\partial \bar{y}'} \right)^2 + \left( \frac{\partial \hat{u}}{\partial \bar{z}'} \right)^2 \right] d\bar{y}' d\bar{z}' \quad (19)$$

wherein the Green's function is

$$G(\bar{y}, \bar{z}, \hat{x} | \bar{y}', \bar{z}', \xi) = \sum_{m=1}^N \left[ \sum_{i=1}^N p_{mi} f_i(\bar{y}', \bar{z}') \right] \Psi_m(\bar{y}, \bar{z}) e^{-\lambda_m^2 (\hat{x} - \xi)}. \quad (20)$$

This form of the Green's function contains the basis functions  $f_i(\bar{y}', \bar{z}')$ , eigenfunctions  $\Psi_m(\bar{y}, \bar{z})$ , parameters  $p_{mi}$ , and eigenvalues  $\lambda_m^2$ . The second contribution, following substitution for the Green's function, attains a standard form,

$$\Phi_2(\bar{y}, \bar{z}; \hat{x}) = \sum_{m=1}^N A_m \Psi_m(\bar{y}, \bar{z}) \frac{1 - e^{-\lambda_m^2 \hat{x}}}{\lambda_m^2} \quad (21)$$

where

$$A_m = \sum_{i=1}^N p_{mi} \int_{\bar{z}=0}^{\bar{b}} \int_{\bar{y}=0}^1 \left[ \frac{\hat{u}^2}{M Da} + \left( \frac{\partial \hat{u}}{\partial \bar{y}'} \right)^2 + \left( \frac{\partial \hat{u}}{\partial \bar{z}'} \right)^2 \right] f_i(\bar{y}', \bar{z}') d\bar{y}' d\bar{z}' \quad (22)$$

It is to be noted that as  $\hat{x}$  becomes large, the solution for  $\Phi_2$  approaches that for the quasi thermally fully developed solution  $\Phi_{2,FD}$ . Therefore, the solution using equation

$$\Phi_2(\bar{y}, \bar{z}; \hat{x}) = \Phi_{2,FD} - \sum_{m=1}^N A_m \Psi_m(\bar{y}, \bar{z}) \frac{e^{-\lambda_m^2 \hat{x}}}{\lambda_m^2} \quad (23)$$

exhibits better convergence characteristics. The solution for  $\Phi_{2,FD}$  uses the Poisson's equation

$$\frac{\partial^2 \Phi_{2,FD}}{\partial \bar{y}^2} + \frac{\partial^2 \Phi_{2,FD}}{\partial \bar{z}^2} + Br \left[ \frac{\hat{u}^2}{M Da} + \left( \frac{\partial \hat{u}}{\partial \bar{y}} \right)^2 + \left( \frac{\partial \hat{u}}{\partial \bar{z}} \right)^2 \right] - S^* \hat{u} = 0 \quad (24a)$$

where

$$S^* = \int_{\bar{z}=0}^{\bar{b}} \int_{\bar{y}=0}^1 \left[ \frac{\hat{u}^2}{M Da} + \left( \frac{\partial \hat{u}}{\partial \bar{y}'} \right)^2 + \left( \frac{\partial \hat{u}}{\partial \bar{z}'} \right)^2 \right] d\bar{y}' d\bar{z}' \quad (24b)$$

and it is obtainable by different methods. Since symbolic algebra is being used, it is determined by the classical Galerkin method [31]. Alternatively, a known  $\Phi_{2,FD}$  solution leads to an initial value problem similar to that used to obtain  $\Phi_1$  instead of the second term on the right side of Eq. (23).

Once the functions  $\Phi_1(\bar{y}, \bar{z}; \hat{x})$  and  $\Phi_2(\bar{y}, \bar{z}; \hat{x})$  are known, the temperature solution  $\theta(\bar{y}, \bar{z}; \hat{x})$  is available. Accordingly, for convenience of this presentation, the two contributions of the dimensionless temperature  $\theta(\bar{y}, \bar{z}; \hat{x}) = \theta_1(\bar{y}, \bar{z}; \hat{x}) + \theta_2(\bar{y}, \bar{z}; \hat{x})$  are presented separately; that is,

$$\theta_1(\bar{y}, \bar{z}; \hat{x}) = \frac{\bar{y}^2}{2} + \frac{\bar{z}^2}{2b} + \Phi_1(\bar{y}, \bar{z}; \hat{x}) \quad (25-a)$$

and

$$\theta_2(\bar{y}, \bar{z}; \hat{x}) = Br \Phi_2(\bar{y}, \bar{z}; \hat{x}). \quad (25-b)$$

Therefore, for  $i=1$  or  $2$ , the following equation provides the mean wall temperature for each contribution,

$$\theta_{i,w}(\hat{x}) = \frac{1}{1+b} \left[ \int_{\bar{y}=0}^1 \theta_i(\bar{y}, \bar{b}; \hat{x}) d\bar{y} + \int_{\bar{z}=0}^{\bar{b}} \theta_i(1, \bar{z}; \hat{x}) d\bar{z} \right] \quad (26)$$

### 2.3 Second Law analysis

Cross-sectional average of the entropy generation rate  $\dot{S}_{gen}$  can be found as [12]

$$d\dot{S}_{gen} = \dot{m}ds - \frac{\delta Q}{T_w}, \quad (27)$$

Noting that the longitudinal pressure gradient is constant,  $-\frac{dP}{dx} = P^*$ , with  $ds = c_p \frac{dT_b}{T_b} - \frac{dp}{\rho T_b}$  and

$\delta Q = q_w C dx$ , and after some algebraic manipulations one has

$$\frac{d\dot{S}_{gen}}{\dot{m}c_p} = \frac{dT_b}{dx} \frac{dx}{T_b} - \frac{P^* dx}{\rho c_p T_b} - \frac{q_w C dx}{\dot{m}c_p T_w}. \quad (28)$$

On the other hand, the First Law of Thermodynamics for an element reads

$$\frac{dT_b}{dx} = \frac{4q_w(1+\bar{b})a^3 + \mu_e U^2 S^* A}{\dot{m}c_p a^2} = T^* \quad (29)$$

where  $T^*$  is a constant (longitudinal bulk temperature gradient). Solving for the bulk temperature, one has

$$T_b = T^* x + T_i \quad (30)$$

Making use of the above equation in the entropy production formula, Eq. (28), one concludes that

$$\frac{d\dot{S}_{gen}}{\dot{m}c_p} = \frac{dx}{x + T_i/T^*} + \frac{P^*}{\rho c_p T^*} \frac{dx}{x + T_i/T^*} - \frac{q_w C dx}{\dot{m}c_p T_w} \quad (31)$$

As the wall temperature is not explicitly defined in terms of the known variables, one replaces it by the dimensionless variable counterpart  $\theta_w = (T_w - T_i)/(q_w a / k_e)$  where, in terms of the tabulated data, one has

$$T_w = T_i + (\theta_{1w} + Br\Phi_{1w}) q_w a / k_e \quad (32)$$

leading to

$$\frac{d\dot{S}_{gen}}{\dot{m}c_p} = \frac{dx}{x + T_i/T^*} + F \frac{dx}{x + T_i/T^*} - \frac{q'' C}{\dot{m}c_p T_i} \frac{dx}{1 + (\theta_{1w} + Br\Phi_{1w}) q^*} \quad (33)$$

with the dimensionless wall heat flux being defined as  $q^* = q_w a / (k_e T_i)$ . Moreover, the dimensionless parameter  $F = P^* / (\rho c_p T^*)$  is a measure of required pumping power to enthalpy change (longitudinal heat transfer). For non-zero Br values and in terms of the Darcy pressure drop one concludes that

$$F = N^* \frac{Br}{MDa} / \left( \frac{4a}{D_H} + BrS^* \right) \quad (34)$$

where  $N^*$  shows the degree of non-Darcy effects on the longitudinal pressure gradient as  $N^* = P^*/(\mu U / K)$ . For the Darcy flow model  $N^*=1$ . Integrating from  $x=0$  to  $x=L$  and rearranging in terms of known parameters, one has

$$Ns = \frac{\dot{S}_{gen}(L)}{\dot{m}c_p} = \ln \left( 1 + q^* \hat{L} \left( \frac{4a}{D_H} + BrS^* \right) \right)^{1+F} - q^* \frac{4a}{D_H} \int_0^{\hat{L}} \frac{d\hat{x}}{1 + (\theta_{lw} + Br\Phi_{lw})q^*} \quad (35a)$$

As seen, like the left-hand-side term the first two terms in the right-hand-side of Eq. (33) are integrated directly; however, the last term on the right side should be evaluated numerically. Before reporting the numerical results, which are obtained using the trapezoidal rule, two limiting cases, for which approximate closed form solutions are obtained, will be presented. It is assumed that the dimensionless heat flux  $q^*$  is very small compared to unity. Commensurate with that is the constant property assumption similar to [29]. First consider the case of a hyperporous medium for which one has  $MDa=O(1)$ . A quick check of our table 1 shows that for this case  $S^*=O(1)$  so that neglecting the terms smaller than  $O(q^*)$ , like  $q^{*2}$ , one finds that

$$Ns = q^* \hat{L} (F(1 + \bar{b})/\bar{b} + BrS^*(1 + F)) \quad (35b)$$

Replacing  $F$ , one has

$$Ns = q^* \hat{L} Br (S^* + N/(MDa)) \quad (35c)$$

Comparing the predictions of the above equation and the numerically obtained results, a good degree of agreement is observed. For example with  $b/a=1$ ,  $N^*=0.1$ , and  $MDa=1$ , Eq. (35c) predicts  $Ns=0.4291$  and  $0.0429$  while the numerical results are  $0.3435$  and  $0.0418$  for  $q^*=0.01$  and  $0.001$ , respectively. The results agree better for smaller  $q^*$  values, as expected based on our asymptotic analysis assumptions.

It is instructive to rearrange Eq. (35c) in terms of dimensional variables as

$$\dot{S}_{gen} = AL \frac{\mu_e U^2}{a^2 T_i} \left( S^* + \frac{N}{MDa} \right) \quad (35d)$$

Based on table 1 results,  $S^*$  decreases with the aspect ratio so that, as shown by Eq. (35d), the square cross-section is associated with the highest entropy generation rate compared to rectangular counterparts.

Another case of interest is the one for which  $MDa \rightarrow 0$  where even for relatively small  $q^*$  one can still expect that the product of  $Brq^*S^*$  will be notably greater than  $O(1)$  so that the second term in the right side of Eq. (35a) is negligible compared to the first one; a term that can be simplified in such a way that  $Ns$  be obtained as

$$Ns = \left( 1 + \frac{N}{MDaS^*} \right) \ln \left( \frac{\mu_e U}{\rho c_p T_i a} \frac{L}{a} S^* \right) \quad (35e)$$

similar to the previous case, Eq. (35e) has been verified versus numerical counterparts for  $MDa=10^{-4}$  and  $N^*=1$  with the other parameters remaining the same. The numerical results are  $Ns=12.249, 7.814$  while approximate counterparts are 12.344 and 7.785 for  $q^*=0.01$  and 0.001, respectively.

### 3. Results and Discussion

In the absence of frictional heating contribution, under the constant wall heat flux condition, the energy balance leads to a relation for the bulk temperature,

$$\theta_{1,b} = (1 + \bar{b})\hat{x}/\bar{b} \quad (36a)$$

The bulk temperature is also obtainable analytically from Eq. (11), with  $\theta(\bar{y}, \bar{z}; \hat{x})$  from Eq. (16). This was done mainly for the verification of the mathematical relations for the temperature solution. Similarly, the application of energy balance to a material element yields the relation

$$\Phi_{2,b} = S^* \hat{x} \quad (36b)$$

and  $S^*$  values for selected values of  $b/a$  and  $MDa$  values are in Table 1.

If one designates  $\theta_w = (T_w - T_i)/(q_w a / k_e)$  and  $\theta_b = (T_b - T_i)/(q_w a / k_e)$ , the Nusselt number is obtainable from the relation  $Nu = ha/k_e = 1/(\theta_w - \theta_b)$  and then using the hydraulic diameter  $D_h = 4ab/(a + b)$  in the definition, the Nusselt number becomes

$$Nu_D = \frac{D_h}{a} Nu = \frac{4\bar{b}}{1 + \bar{b}} \left( \frac{1}{\theta_w - \theta_b} \right) = \frac{4\bar{b}}{1 + \bar{b}} \left[ \frac{1}{(\theta_{1,w} - \theta_{1,b}) + Br(\Phi_{2,w} - \Phi_{2,b})} \right]. \quad (37)$$

The values of  $Nu_D$  can be determined from tabulated  $(\theta_{1,w} - \theta_{1,b})$  and  $(\Phi_{2,w} - \Phi_{2,b})$  data in Tables 2(a,b) through 5(a,b), at different  $\hat{x} = (x/a)/Pe$ ,  $b/a$ ,  $MDa$ , and  $Br$  values which can be positive or negative depending on the direction of heat flux.

The data for  $\Phi_{2,w} - \Phi_{2,b}$  can also identify the values of the wall temperature in the absence of heating or cooling at the walls where viscous dissipation is the only reason for heat transfer as discussed by Hooman et al. [24] for a similar problem with isothermal wall heating. In this case the energy generated inside the duct should be carried by the moving fluid leading to an increase in the fluid enthalpy. For this case one obtains the wall and bulk temperature as

$$\frac{T_w(y, z; x) - T_i}{\mu_e U^2 / k_e} = \Phi_{2,w}(\bar{y}, \bar{z}; \hat{x}), \quad (38-a)$$

$$\frac{T_b(y, z; x) - T_i}{\mu_e U^2 / k_e} = \Phi_{2,b}(\bar{y}, \bar{z}; \hat{x}) = S^* \hat{x}. \quad (38-b)$$

One notes that the temperature scale is  $\mu_e U^2 / k_e$  for this case as there is no wall heat flux to be included in the denominator. The data in Tables 2(a,b) through 5(a,b) can be used to illustrate the wall-bulk temperature difference  $\Phi_{2,w} - \Phi_{2,b}$ . This has been done for some cases as shown in Figures 2(a-d) for  $b/a=1, 2, 4,$  and  $10$  where the variations of the wall temperature  $\theta_{1,w}$  and the bulk temperature  $\theta_{1,b}$  are graphically presented in [21] for the same aspect ratios. As a common trend in all charts on Figures 2(a-d), one observes that value of  $\Phi_{2,w} - \Phi_{2,b}$  increases along the duct. However, with  $MDa > 0.1$  the curve experiences a turning point while for smaller values of  $MDa$  there is a sharp increase in  $\Phi_{2,w} - \Phi_{2,b}$ .

For a more comprehensive analysis of the problem, one can use the data presented in tables 1-5 to find the Nusselt number for any arbitrary combination of the key parameters. As an illustration, this is partly done and the results are in Figures 3-4. Figure 3(a) shows the developing Nusselt number for  $MDa=0.001$  versus the streamwise direction for several values of  $Br$ . It is clear that increasing  $Br$  will reduce the Nusselt number level. Moreover, increasing  $Br$  and aspect ratio, the  $Nu_D-x$  plots tend to be more flattened. The square cross-section seems to behave differently for higher  $Br$  values in such a way that the developing Nusselt number is as high as that of other aspect ratios in the duct entrance and then decreases sharply with the fully developed  $Nu_D$  being the minimum among the other counterparts. It is interesting that in their study of heat transfer and entropy generation in a duct of rectangular cross-section with the fully developed assumption, Hooman et al. [29] have reported that the square cross-section acts in a different manner for very small  $MDa$  values where the velocity profile is nearly slug and the problem is a conduction-like one. They attributed this fact (in part) to the special geometry of a square for having more symmetry compared to rectangular counterparts. Figure 3(b) shows  $Nu_D$  versus longitudinal coordinate for different  $Br$  values with  $MDa=1$  which represents a hyperporous medium. It can be concluded that for a fixed  $Br$  value  $Nu_D$  increases with the aspect ratio for all cases considered here.

Figures 4(a,b) present the fully developed  $Nu_D$  versus  $Br$  for two limiting aspect ratios being  $b/a=1$  and  $10$ . One realizes that the hyperporous case, with  $MDa=1$ , mimics the clear fluid counterpart as the corresponding curves are nearly identical but moving from  $MDa=0.0001$  to  $0.001$ , changes in the Nusselt number are more pronounced compared to the former case. In line with the aforementioned observations increasing  $Br$  or decreasing  $MDa$  will decrease the Nusselt number for either values of the duct aspect ratio. Moreover, the Nusselt number puts higher values for smaller aspect ratio compared to the higher one. Nevertheless, it should be noted that, for small  $Br$  values, selection of a length scale in the Nusselt number (hydraulic diameter) is partly responsible for that similar to what was reported by [29]. Interestingly, moving to higher  $Br$  values, this choice becomes of less importance.

For a better understanding of the problem, Eq. (37) is rearranged in terms of the Nusselt number for negligible viscous dissipation case,  $Nu^*$ , as follows

$$Nu_D = \frac{4\bar{b}}{1+\bar{b}} \left[ \frac{1}{Nu^*} + Br(\Phi_{2,w} - \Phi_{2,b}) \right]^{-1}. \quad (39)$$

Eq. (39) is identical to the form reported by Kakaç et al. [33] for clear flow through a pipe and also by Hooman and Gurgenci [34] for a parallel plate porous channel (see [35-37] for more closed form solutions for similar problems), if rearranged as follows

$$Nu_D = \frac{4\bar{b}}{1+\bar{b}} \left[ \frac{Nu^*}{1 + Nu^* Br(\Phi_{2,w} - \Phi_{2,b})} \right]. \quad (40)$$

It is an easy task to see that increasing  $Br$  decreases  $Nu_D$  where  $Nu^*$  is the Nusselt number for the case where one can neglect the viscous dissipation effects. Eq. (40) can be modified to be used for ducts of other cross-sections. The significance of this point becomes more vivid as one can apply Eq. (40) to account for the viscous dissipation effects, for the fully developed or thermally developing region, by combining two easier problems, with their answers available in the literature, to obtain the solution to a more complex problem. For example one can use the correlations proposed by Haji-Sheikh [38] to find  $Nu^*$  for ducts of parallel plate or circular cross-sections and solve only for the second part to obtain the final solution for a problem where frictional heating is important. This seems to be of practical importance in engineering applications where usually one is in search for a rough and ready estimate rather than complicated calculations.

It is worth noting that several combinations of the key parameters can lead to different results, based on the data in tables 2-5; however, for the sake of brevity, we restrict our results for the Second Law aspects of the problem to the most irreversible geometry being the square cross-section (see [11-13] and [29]). Figure 5 illustrates plots of  $Ns$  versus  $Br$  for two different values of  $MDa$  being 1 and  $10^{-4}$ . As seen, with the other parameters fixed, decreasing  $MDa$  or increasing either of  $Br$  or  $q^*$  increases the entropy production rate. This is inline with the results of Hooman et al. [29]. Moving from  $MDa=1$  to  $10^{-4}$ , the  $Ns$ - $Br$  slope changes as expected based on the approximate predictions of Eq. (35d-e).

#### 4. Conclusion

The effect of viscous dissipation on heat transfer and entropy generation for thermally developing forced convection in a porous-saturated duct of rectangular cross-section is investigated. The classical Galerkin method is applied to solve the Brinkman momentum equation while the EWRM is undertaken to solve the non-homogenous three-dimensional thermal energy equation. It is believed that the solution reported in this study can serve as a benchmark for verification of numerical solutions concerning similar



problems [39-46]. It was observed that viscous dissipation reduces the Nusselt number in both thermally developing and fully developed regions unlike the similar case with isothermal wall heating. Key parameters affecting the Second Law aspects of the problem are highlighted and analyzed.

### **Acknowledgments**

The first author, the scholarship holder, acknowledges the financial support provided by The University of Queensland in terms of UQILAS, Endeavor IPRS, and School Scholarship.

### **References**

- [1] D.A. Nield, A. Bejan, *Convection in Porous Media*, 3rd ed., Springer, New York, 2006.
- [2] H. I. Ene, E. Sanchez-Palencia, On thermal equation for flow in porous media, *Int. J. Engng. Sci.* 20 (1982) 623–630.
- [3] D. A. Nield, Resolution of a paradox involving viscous dissipation and nonlinear drag in a porous medium, *Transport Porous Media* 41 (2000) 349-357.
- [4] A. K. Al-Hadhrami, L. Elliot, D. B. Ingham, A new model for viscous dissipation in porous media across a range of permeability values, *Transport Porous Media* 53 (2003) 117-122.
- [5] W. P. Breugem, D.A.S. Rees, A derivation of the volume-averaged Boussinesq equations for flow in porous media with viscous dissipation, *Transport Porous Media* (2006) 63: 1–12.
- [6] D.A. Nield, Modelling fluid flow in saturated porous media and at interfaces, in *Transport Phenomena in Porous Media II* (D. B. Ingham and I. Pop, eds.), Elsevier Science, Oxford, 2002.
- [7] D.A. Nield, A note on a Brinkman-Brinkman forced convection problem, *Transport Porous Media* 64 (2006) 185–188
- [8] D. Bercovici, Generation of plate tectonics from lithosphere–mantle flow and void-volatile self-lubrication, *Earth Planetary Science Letters* 154 (1998) 139–151.
- [9] G. P. Celata, G. L. Morini, V. Marconi, S.J. McPhail, G. Zummo, Using viscous heating to determine the friction factor in microchannels - An experimental validation, *Experimental Thermal Fluid Sci.* 30 (2006) 725-731.
- [10] Y. Murakami, B. Mikic, Parametric investigation of viscous dissipation effects on optimized air cooling microchanneled heat sinks, *Heat Transfer Engng.*, 24 (2003) 53-62.
- [11] A. Bejan, *Entropy Generation through Heat and Fluid Flow*, Wiley, New York, 1982.
- [12] A.Z. Sahin, Irreversibilities in various duct geometries with constant wall heat flux and laminar flow, *Energy* 23 (1998) 465-473
- [13] E.B. Ratts, A.G. Raut, Entropy generation minimization of fully developed internal flow with constant heat flux, *ASME J. Heat Transfer* 126 (2004) 656-659.

- [14] A.C. Baytas, Entropy generation for free and forced convection in a porous cavity and a porous channel, in *Emerging Technology and Techniques in Porous Media* (Eds. D.B. Ingham et al.), Kluwer Academic Publishers (2004) 259-270.
- [15] K. Hooman, A. Ejlali, Entropy generation for forced convection in a porous saturated circular tube with uniform wall temperature, *Int. Comm. Heat Mass Transfer* 34 (2007) 408-419.
- [16] K. Hooman, Entropy-energy analysis of forced convection in a porous-saturated circular tube considering temperature-dependent viscosity effects, *Int. J. Exergy* 3 (2006) 436–451.
- [17] K. Hooman, A. Ejlali, Second law analysis of laminar flow in a channel filled with saturated porous media: a numerical solution, *Entropy*, 7 (2005) 300-307.
- [18] A. Haji-Sheikh, K. Vafai, Analysis of flow and heat transfer in porous media imbedded inside various-shaped ducts, *Int. J. Heat Mass Transfer* 47 (2004) 1889-1905.
- [19] A. Haji-Sheikh, Fully developed heat transfer to fluid flow in rectangular passages with filled with porous materials, *ASME J. Heat Transfer* 128 (2006) 822–828.
- [20] A. Haji-Sheikh, W. J. Minkowycz, E. M. Sparrow, Green's function solution of temperature field for flow in porous passages, *Int. J. Heat Mass Transfer* 47 (2004) 4685-4695.
- [21] A. Haji-Sheikh, D. A. Nield, K. Hooman, Heat transfer in thermal entrance region for flow through rectangular porous passages, *Int. J. Heat Mass Transfer* 49 (2006) 3004–3015
- [22] A. Haji-Sheikh, W. J. Minkowycz, E. M. Sparrow, A numerical study of the heat transfer to fluid flow through circular porous passages, *Num. Heat Transfer A* 46 (2004) 929-955.
- [23] A. Haji-Sheikh, E. M. Sparrow, W. J. Minkowycz, Heat transfer to flow through porous passages using extended weighted residuals method—A Green's function solution, *Int. J. Heat Mass Transfer* 48 (2005) 1330-1349.
- [24] K. Hooman, A. Haji-Sheikh, D.A. Nield, Thermally developing Brinkman-Brinkman forced convection in rectangular ducts with isothermal walls, *Int. J. Heat Mass Transfer*, in press.
- [25] K. Hooman, A.A. Merrikh, Analytical solution of forced convection in a duct of rectangular cross-section saturated by a porous medium, *ASME J. Heat Transfer*, 128 (2006) 596-600.
- [26] K. Hooman, H. Gurgenci, Effects of temperature-dependent viscosity variation on entropy generation, heat, and fluid flow through a porous-saturated duct of rectangular cross-section, *Appl. Math. Mech.* 28 (2007) 69-78
- [27] K. Hooman, Fully developed temperature distribution in porous saturated duct of elliptical cross-section, with viscous dissipation effects and entropy generation analysis, *Heat Transfer Research* 36 (2005) 237-245.
- [28] K. Hooman, Analysis of entropy generation in porous media imbedded inside elliptical passages, *Int. J. Heat Technology* 23 (2005) 145-149.

- [29] K. Hooman, H. Gurgenci, A.A., Merrikh, Heat transfer and entropy generation optimization of forced convection in a porous-saturated duct of rectangular cross-section, *International Journal of Heat and Mass Transfer* 50 (2007) 2051-2059.
- [30] R.K. Shah, A.L. London, *Laminar Flow Forced Convection in Ducts (Advances in Heat Transfer, Supplement 1)*, Academic Press, New York, 1978.
- [31] L. V. Kantorovich and V. I. Krylov, *Approximate Methods of Higher Analysis*, Wiley, New York, 1960.
- [32] J.V. Beck, K. Cole, A. Haji-Sheikh, B. Litkouhi, *Heat Conduction Using Green's Functions*, Hemisphere Publ. Corp., Washington D. C., 1992.
- [33] S. Kakaç, R.K. Shah, W. Aung, *Handbook of Single-Phase Convective Heat Transfer*, Wiley, New York, 1987.
- [34] K. Hooman, H. Gurgenci, Effects of viscous dissipation and boundary conditions on forced convection in a channel occupied by a saturated porous medium, *Transport in Porous Media* (2007), doi:10.1007/s11242-006-9049-4
- [35] D.A. Nield, A.V. Kuznetsov, M. Xiong, Effects of viscous dissipation and flow work on forced convection in a channel filled by a saturated porous medium, *Transport Porous Media* 56 (2004) 351-367.
- [36] D. A. Nield, K. Hooman, Comments on "Effects of viscous dissipation on the heat transfer in forced pipe flow. Part 1: both hydrodynamically and thermally fully developed flow, and Part 2: thermally developing flow" by O. Aydin, *Energy Conv. Manag.*, 47 (2006) 3501-3503.
- [37] K. Hooman, A. Pourshaghaghay, A. Ejlali, Effects of viscous dissipation on thermally developing forced convection in a porous saturated circular tube with an isoflux wall, *Appl. Math. Mech.* 27 (2006) 617-626.
- [38] A. Haji-Sheikh, Estimation of average and local heat transfer in parallel plates and circular ducts filled with porous materials, *ASME J. Heat Transfer* 126 (2004) 400-409.
- [39] A.R.A. Khaled, K. Vafai, Analysis of flow and heat transfer inside nonisothermal squeezed thin films, *Numerical Heat Transfer Part A*, 47 (10) (2005) 981-996.
- [40] S. V. Iyer, K. Vafai, Passive heat transfer augmentation in a cylindrical annulus utilizing a porous perturbation, *Numerical Heat Transfer Part A*, 36 (2) (1999) 115-128.
- [41] S.S. Mousavi, K. Hooman, Heat and fluid flow in entrance region of a channel with staggered baffles, *Energy Conversion and Management*, 47 (15-16) (2006) 2011-2019
- [42] K. Khanafer, K. Vafai, Double-diffusive mixed convection in a lid-driven enclosure filled with a fluid-saturated porous medium, *Numerical Heat Transfer Part A*, 42 (5) (2002) 465-486.
- [43] K. Hooman, A perturbation solution for forced convection in a porous-saturated duct, *J. Comput. Appl. Math.* (2006), doi: 10.1016/j.cam.2006.11.005

[44] A. Narasimhan, J. L. Lage, Forced convection of a fluid with temperature-dependent viscosity flowing through a porous medium channel, Numerical Heat Transfer Part A, 40 (2001): 801-820.

[45] S. C. Chen, K. Vafai, Non-Darcian surface tension effects on free surface transport in porous media Numerical Heat Transfer Part A, 31 (1997) 235-254.

[46] P. C. Huang, K. Vafai, Internal heat transfer augmentation in a channel using an alternate set of porous cavity-block obstacles, Numerical Heat Transfer Part A, 25 (1994) 519-539.

Table 1. The parameter  $S^*$ , for different  $b/a$  and  $MDa$  values, for determination of  $\Phi_{2,b} = S^* \cdot \hat{x}$ .

$MDa$	$b/a=1$	$b/a=2$	$b/a=4$	$b/a=10$
0.0001	10202.9	10151.6	10126.3	10111.5
0.001	1066.07	1049.09	1040.81	1035.90
0.01	123.042	116.772	113.871	112.199
0.1	20.1833	16.9485	15.6872	15.0167
1	8.48230	5.70568	4.83563	4.42943
10	7.25128	4.50748	3.68970	3.32534
$\infty$	7.11354	4.37289	3.56109	3.20179

Table 2(a). The difference between the dimensionless wall temperature and bulk temperature due to the wall effect and frictional heating contribution when  $b/a = 1$ .

$\hat{x}$	$M Da = \infty$		$M Da = 1$		$M Da = 1/10$	
	$\theta_{1,w}-\theta_{1,b}$	$\Phi_{2,w}-\Phi_{2,b}$	$\theta_{1,w}-\theta_{1,b}$	$\Phi_{2,w}-\Phi_{2,b}$	$\theta_{1,w}-\theta_{1,b}$	$\Phi_{2,w}-\Phi_{2,b}$
0.0005	0.0949	0.044	0.0928	0.046	0.0816	0.061
0.0006	0.1012	0.049	0.0990	0.051	0.0870	0.068
0.0008	0.1119	0.058	0.1095	0.061	0.0963	0.080
0.001	0.1211	0.067	0.1184	0.070	0.1043	0.090
0.002	0.1545	0.102	0.1512	0.106	0.1333	0.132
0.003	0.1783	0.131	0.1745	0.134	0.1540	0.163
0.004	0.1971	0.155	0.1930	0.159	0.1705	0.189
0.005	0.2130	0.176	0.2086	0.180	0.1844	0.212
0.006	0.2269	0.196	0.2223	0.200	0.1966	0.231
0.008	0.2505	0.231	0.2454	0.235	0.2174	0.265
0.01	0.2703	0.262	0.2649	0.265	0.2348	0.294
0.02	0.3402	0.381	0.3337	0.382	0.2969	0.397
0.03	0.3868	0.469	0.3796	0.468	0.3386	0.467
0.04	0.4219	0.540	0.4143	0.536	0.3703	0.519
0.05	0.4499	0.600	0.4420	0.592	0.3958	0.561
0.06	0.4731	0.650	0.4649	0.641	0.4169	0.596
0.08	0.5095	0.733	0.5010	0.719	0.4502	0.651
0.1	0.5369	0.798	0.5280	0.780	0.4753	0.692
0.2	0.608	0.974	0.5984	0.947	0.5406	0.802
0.3	0.633	1.039	0.6231	1.007	0.5632	0.840
0.4	0.6422	1.063	0.6322	1.029	0.5714	0.854
0.5	0.6457	1.072	0.6356	1.038	0.5744	0.859
0.6	0.6470	1.075	0.6369	1.041	0.5755	0.861
0.8	0.6477	1.077	0.6376	1.042	0.5760	0.862
1	0.6478	1.077	0.6377	1.043	0.5761	0.862
2	0.6478	1.077	0.6377	1.043	0.5761	0.862
3	0.6478	1.077	0.6377	1.043	0.5761	0.862
4	0.6478	1.077	0.6377	1.043	0.5761	0.862
5	0.6478	1.077	0.6377	1.043	0.5761	0.862

Table 2(b). The difference between the dimensionless wall temperature and bulk temperature due to the wall effect and frictional heating contribution when  $b/a = 1$ .

$\hat{x}$	$Ma = 1/100$		$Ma = 1/1000$		$Ma = 1/10000$	
	$\theta_{1,w}-\theta_{1,b}$	$\Phi_{2,w}-\Phi_{2,b}$	$\theta_{1,w}-\theta_{1,b}$	$\Phi_{2,w}-\Phi_{2,b}$	$\theta_{1,w}-\theta_{1,b}$	$\Phi_{2,w}-\Phi_{2,b}$
0.0005	0.0609	0.132	0.0441	0.132	0.0441	0.274
0.0006	0.0647	0.143	0.0471	0.143	0.0471	0.292
0.0008	0.0714	0.162	0.0521	0.162	0.0521	0.313
0.001	0.0773	0.177	0.0564	0.177	0.0564	0.325
0.002	0.0991	0.234	0.0727	0.234	0.0727	0.345
0.003	0.1146	0.272	0.0847	0.272	0.0847	0.354
0.004	0.1271	0.300	0.0944	0.300	0.0944	0.360
0.005	0.1376	0.322	0.1028	0.322	0.1028	0.364
0.006	0.1469	0.341	0.1102	0.341	0.1102	0.367
0.008	0.1627	0.370	0.1229	0.370	0.1229	0.371
0.01	0.1761	0.392	0.1337	0.392	0.1337	0.374
0.02	0.2240	0.459	0.1733	0.459	0.1733	0.381
0.03	0.2565	0.494	0.2009	0.494	0.2009	0.383
0.04	0.2814	0.517	0.2223	0.517	0.2223	0.385
0.05	0.3016	0.533	0.2398	0.533	0.2398	0.386
0.06	0.3185	0.546	0.2545	0.546	0.2545	0.386
0.08	0.3453	0.564	0.2783	0.564	0.2783	0.387
0.1	0.3658	0.577	0.2966	0.577	0.2966	0.388
0.2	0.4197	0.608	0.3461	0.608	0.3461	0.389
0.3	0.4383	0.618	0.3638	0.618	0.3638	0.389
0.4	0.4448	0.622	0.3701	0.622	0.3701	0.389
0.5	0.4471	0.623	0.3725	0.623	0.3725	0.389
0.6	0.4479	0.624	0.3733	0.624	0.3733	0.389
0.8	0.4483	0.624	0.3737	0.624	0.3737	0.389
1	0.4484	0.624	0.3738	0.624	0.3738	0.389
2	0.4484	0.624	0.3738	0.624	0.3738	0.389
3	0.4484	0.624	0.3738	0.624	0.3738	0.389
4	0.4484	0.624	0.3738	0.624	0.3738	0.389
5	0.4484	0.624	0.3738	0.624	0.3738	0.389

Table 3(a). The difference between the dimensionless wall temperature and bulk temperature due to the wall effect and frictional heating contribution when  $b/a = 2$ .

$\hat{x}$	$Ma = \infty$		$Ma = 1$		$Ma = 1/10$	
	$\theta_{1,w}-\theta_{1,b}$	$\Phi_{2,w}-\Phi_{2,b}$	$\theta_{1,w}-\theta_{1,b}$	$\Phi_{2,w}-\Phi_{2,b}$	$\theta_{1,w}-\theta_{1,b}$	$\Phi_{2,w}-\Phi_{2,b}$
0.0005	0.0995	0.034	0.0964	0.037	0.0819	0.054
0.0006	0.1059	0.038	0.1027	0.041	0.0875	0.060
0.0008	0.1170	0.045	0.1134	0.049	0.0968	0.070
0.001	0.1264	0.052	0.1224	0.056	0.1046	0.080
0.002	0.1611	0.080	0.1558	0.085	0.1329	0.116
0.003	0.1855	0.103	0.1795	0.108	0.1532	0.143
0.004	0.2051	0.122	0.1985	0.128	0.1695	0.165
0.005	0.2218	0.139	0.2145	0.145	0.1834	0.185
0.006	0.2363	0.155	0.2286	0.161	0.1955	0.202
0.008	0.2610	0.182	0.2526	0.189	0.2161	0.231
0.01	0.2819	0.207	0.2728	0.214	0.2335	0.256
0.02	0.3564	0.303	0.3452	0.309	0.2963	0.344
0.03	0.4071	0.374	0.3946	0.378	0.3392	0.402
0.04	0.4463	0.432	0.4327	0.433	0.3724	0.446
0.05	0.4783	0.480	0.4638	0.479	0.3996	0.481
0.06	0.5054	0.522	0.4902	0.519	0.4227	0.510
0.08	0.5495	0.591	0.5331	0.584	0.4602	0.555
0.1	0.5845	0.646	0.5671	0.635	0.4898	0.590
0.2	0.6922	0.808	0.6713	0.784	0.5792	0.683
0.3	0.7496	0.883	0.7264	0.852	0.6248	0.722
0.4	0.7860	0.925	0.7610	0.888	0.6527	0.740
0.5	0.8110	0.951	0.7848	0.911	0.6717	0.751
0.6	0.8291	0.968	0.8020	0.926	0.6855	0.758
0.8	0.8524	0.990	0.8243	0.945	0.7033	0.766
1	0.8656	1.003	0.8369	0.955	0.7136	0.771
2	0.8822	1.018	0.8529	0.969	0.7270	0.777
3	0.8832	1.019	0.8539	0.969	0.7279	0.778
4	0.8832	1.019	0.8539	0.970	0.7280	0.778
5	0.8832	1.019	0.8539	0.970	0.7280	0.778

Table 3(b). The difference between the dimensionless wall temperature and bulk temperature due to the wall effect and frictional heating contribution when  $b/a = 2$ .

$\hat{x}$	$MDa = 1/100$		$MDa = 1/1000$		$MDa = 1/10000$	
	$\theta_{1,w}-\theta_{1,b}$	$\Phi_{2,w}-\Phi_{2,b}$	$\theta_{1,w}-\theta_{1,b}$	$\Phi_{2,w}-\Phi_{2,b}$	$\theta_{1,w}-\theta_{1,b}$	$\Phi_{2,w}-\Phi_{2,b}$
0.0005	0.0591	0.123	0.0423	0.252	0.0334	0.285
0.0006	0.0633	0.134	0.0454	0.269	0.0361	0.296
0.0008	0.0706	0.154	0.0508	0.295	0.0407	0.312
0.001	0.0767	0.169	0.0554	0.314	0.0446	0.324
0.002	0.0983	0.223	0.0726	0.366	0.0595	0.352
0.003	0.1133	0.258	0.0848	0.391	0.0703	0.362
0.004	0.1254	0.285	0.0945	0.408	0.0792	0.367
0.005	0.1358	0.305	0.1028	0.420	0.0868	0.370
0.006	0.1450	0.323	0.1101	0.429	0.0937	0.372
0.008	0.1607	0.350	0.1229	0.442	0.1057	0.376
0.01	0.1740	0.370	0.1339	0.452	0.1161	0.378
0.02	0.2222	0.432	0.1747	0.475	0.1550	0.382
0.03	0.2556	0.464	0.2036	0.486	0.1829	0.383
0.04	0.2816	0.485	0.2264	0.492	0.2050	0.384
0.05	0.3031	0.500	0.2454	0.496	0.2235	0.384
0.06	0.3214	0.511	0.2617	0.500	0.2394	0.383
0.08	0.3513	0.528	0.2887	0.504	0.2657	0.383
0.1	0.3751	0.539	0.3103	0.507	0.2869	0.382
0.2	0.4472	0.568	0.3767	0.515	0.3522	0.380
0.3	0.4833	0.578	0.4103	0.517	0.3853	0.378
0.4	0.5050	0.583	0.4304	0.519	0.4051	0.377
0.5	0.5196	0.586	0.4438	0.519	0.4182	0.376
0.6	0.5301	0.587	0.4535	0.520	0.4277	0.375
0.8	0.5440	0.589	0.4663	0.520	0.4402	0.374
1	0.5522	0.590	0.4739	0.521	0.4476	0.374
2	0.5633	0.592	0.4845	0.521	0.4582	0.373
3	0.5642	0.592	0.4854	0.521	0.459	0.373
4	0.5642	0.592	0.4854	0.521	0.4591	0.373
5	0.5642	0.592	0.4854	0.521	0.4591	0.373



Table 4(a). The difference between the dimensionless wall temperature and bulk temperature due to the wall effect and frictional heating contribution when  $b/a = 4$ .

$\hat{x}$	$Ma = \infty$		$Ma = 1$		$Ma = 1/10$	
	$\theta_{1,w}-\theta_{1,b}$	$\Phi_{2,w}-\Phi_{2,b}$	$\theta_{1,w}-\theta_{1,b}$	$\Phi_{2,w}-\Phi_{2,b}$	$\theta_{1,w}-\theta_{1,b}$	$\Phi_{2,w}-\Phi_{2,b}$
0.0005	0.0936	0.033	0.0902	0.035	0.0767	0.050
0.0006	0.1002	0.037	0.0965	0.040	0.0819	0.056
0.0008	0.1114	0.044	0.1073	0.047	0.0910	0.067
0.001	0.1209	0.051	0.1165	0.055	0.0988	0.076
0.002	0.1551	0.079	0.1497	0.083	0.1276	0.113
0.003	0.1786	0.101	0.1726	0.106	0.1478	0.140
0.004	0.1970	0.119	0.1904	0.125	0.1636	0.162
0.005	0.2125	0.136	0.2054	0.141	0.1767	0.180
0.006	0.2260	0.151	0.2184	0.157	0.1881	0.197
0.008	0.2490	0.178	0.2407	0.184	0.2074	0.225
0.01	0.2684	0.202	0.2594	0.208	0.2236	0.248
0.02	0.3377	0.293	0.3266	0.298	0.2819	0.333
0.03	0.3849	0.360	0.3723	0.364	0.3218	0.389
0.04	0.4214	0.414	0.4075	0.416	0.3525	0.430
0.05	0.4512	0.459	0.4364	0.459	0.3777	0.463
0.06	0.4765	0.497	0.4608	0.495	0.3990	0.490
0.08	0.5177	0.558	0.5006	0.553	0.4336	0.533
0.1	0.5505	0.606	0.5321	0.599	0.4609	0.565
0.2	0.6530	0.737	0.6295	0.722	0.5429	0.648
0.3	0.7109	0.790	0.6834	0.770	0.5853	0.678
0.4	0.7513	0.815	0.7205	0.792	0.6130	0.691
0.5	0.7830	0.829	0.7493	0.804	0.6341	0.697
0.6	0.8096	0.839	0.7734	0.813	0.6514	0.701
0.8	0.8528	0.853	0.8125	0.824	0.6793	0.706
1	0.8873	0.863	0.8437	0.832	0.7016	0.710
2	0.9921	0.890	0.9385	0.853	0.7702	0.718
3	1.0416	0.901	0.9836	0.863	0.8035	0.721
4	1.0663	0.907	1.0063	0.867	0.8207	0.723
5	1.0787	0.910	1.0177	0.869	0.8296	0.724

Table 4(b). The difference between the dimensionless wall temperature and bulk temperature due to the wall effect and frictional heating contribution when  $b/a = 4$ .

$\hat{x}$	$MDa = 1/100$		$MDa = 1/1000$		$MDa = 1/10000$	
	$\theta_{1,w}-\theta_{1,b}$	$\Phi_{2,w}-\Phi_{2,b}$	$\theta_{1,w}-\theta_{1,b}$	$\Phi_{2,w}-\Phi_{2,b}$	$\theta_{1,w}-\theta_{1,b}$	$\Phi_{2,w}-\Phi_{2,b}$
0.0005	0.0575	0.113	0.0434	0.225	0.0344	0.328
0.0006	0.0610	0.124	0.0462	0.237	0.0368	0.337
0.0008	0.0673	0.143	0.0508	0.257	0.0410	0.352
0.001	0.0728	0.160	0.0549	0.273	0.0447	0.363
0.002	0.0941	0.218	0.0709	0.326	0.0593	0.393
0.003	0.1095	0.254	0.0831	0.356	0.0705	0.405
0.004	0.122	0.281	0.0931	0.377	0.0798	0.412
0.005	0.1324	0.301	0.1017	0.391	0.0877	0.416
0.006	0.1415	0.318	0.1093	0.402	0.0948	0.419
0.008	0.1569	0.344	0.1223	0.418	0.1069	0.423
0.01	0.1697	0.364	0.1333	0.428	0.1173	0.426
0.02	0.2155	0.423	0.1732	0.452	0.1556	0.433
0.03	0.2473	0.454	0.2012	0.462	0.1831	0.437
0.04	0.2721	0.474	0.2235	0.468	0.2050	0.438
0.05	0.2926	0.489	0.2420	0.473	0.2232	0.440
0.06	0.3100	0.500	0.2579	0.476	0.2389	0.440
0.08	0.3384	0.515	0.2842	0.480	0.2649	0.442
0.1	0.3609	0.527	0.3052	0.483	0.2857	0.442
0.2	0.4287	0.553	0.3692	0.491	0.3493	0.444
0.3	0.4628	0.563	0.4014	0.494	0.3814	0.445
0.4	0.4842	0.567	0.4212	0.495	0.4011	0.445
0.5	0.4999	0.569	0.4356	0.495	0.4152	0.445
0.6	0.5126	0.570	0.4471	0.495	0.4264	0.445
0.8	0.5332	0.571	0.4655	0.496	0.4443	0.445
1	0.5497	0.572	0.4802	0.496	0.4586	0.445
2	0.6010	0.573	0.5263	0.497	0.5035	0.445
3	0.6266	0.574	0.5495	0.497	0.5261	0.444
4	0.6401	0.575	0.5618	0.497	0.5381	0.444
5	0.6473	0.575	0.5684	0.497	0.5446	0.444

Table 5(a). The difference between the dimensionless wall temperature and bulk temperature due to the wall effect and frictional heating contribution when  $b/a = 10$ .

$\hat{x}$	$Ma = \infty$		$Ma = 1$		$Ma = 1/10$	
	$\theta_{1,w}-\theta_{1,b}$	$\Phi_{2,w}-\Phi_{2,b}$	$\theta_{1,w}-\theta_{1,b}$	$\Phi_{2,w}-\Phi_{2,b}$	$\theta_{1,w}-\theta_{1,b}$	$\Phi_{2,w}-\Phi_{2,b}$
0.0005	0.0893	0.028	0.0878	0.035	0.0779	0.050
0.0006	0.0947	0.032	0.0930	0.039	0.0824	0.055
0.0008	0.1041	0.039	0.1020	0.047	0.0902	0.065
0.001	0.1122	0.045	0.1096	0.054	0.0969	0.074
0.002	0.1420	0.072	0.1379	0.083	0.1215	0.109
0.003	0.1633	0.094	0.1582	0.106	0.1391	0.135
0.004	0.1803	0.115	0.1745	0.125	0.1533	0.157
0.005	0.1948	0.134	0.1883	0.143	0.1654	0.176
0.006	0.2074	0.151	0.2004	0.158	0.1759	0.193
0.008	0.2287	0.182	0.2211	0.186	0.1941	0.221
0.01	0.2465	0.210	0.2385	0.211	0.2094	0.246
0.02	0.3087	0.311	0.2999	0.303	0.2643	0.332
0.03	0.3498	0.379	0.3407	0.369	0.3012	0.388
0.04	0.3809	0.431	0.3713	0.420	0.3291	0.429
0.05	0.4061	0.473	0.3960	0.462	0.3515	0.462
0.06	0.4272	0.509	0.4166	0.498	0.3702	0.488
0.08	0.4612	0.565	0.4495	0.555	0.4000	0.529
0.1	0.4877	0.609	0.4751	0.598	0.4229	0.560
0.2	0.5651	0.725	0.5492	0.709	0.4880	0.638
0.3	0.6039	0.765	0.5853	0.746	0.5176	0.664
0.4	0.6292	0.781	0.6084	0.761	0.5351	0.673
0.5	0.6490	0.788	0.6262	0.767	0.5479	0.677
0.6	0.6658	0.792	0.6412	0.771	0.5584	0.679
0.8	0.6944	0.798	0.6666	0.775	0.5761	0.682
1	0.7188	0.801	0.6882	0.778	0.5911	0.683
2	0.8082	0.811	0.7673	0.786	0.6459	0.686
3	0.8703	0.815	0.8223	0.790	0.6841	0.688
4	0.9185	0.818	0.8649	0.792	0.7139	0.689
5	0.9579	0.820	0.8997	0.794	0.7383	0.689

Table 5(b). The difference between the dimensionless wall temperature and bulk temperature due to the wall effect and frictional heating contribution when  $b/a = 10$ .

$\hat{x}$	$MDa = 1/100$		$MDa = 1/1000$		$MDa = 1/10000$	
	$\theta_{1,w}-\theta_{1,b}$	$\Phi_{2,w}-\Phi_{2,b}$	$\theta_{1,w}-\theta_{1,b}$	$\Phi_{2,w}-\Phi_{2,b}$	$\theta_{1,w}-\theta_{1,b}$	$\Phi_{2,w}-\Phi_{2,b}$
0.0005	0.0594	0.112	0.0455	0.244	0.0371	0.313
0.0006	0.0628	0.122	0.0481	0.256	0.0394	0.325
0.0008	0.0689	0.140	0.0527	0.275	0.0434	0.341
0.001	0.0740	0.154	0.0567	0.290	0.0469	0.353
0.002	0.0932	0.206	0.0720	0.335	0.0605	0.378
0.003	0.1070	0.239	0.0832	0.360	0.0709	0.387
0.004	0.1182	0.265	0.0925	0.376	0.0796	0.392
0.005	0.1277	0.285	0.1005	0.387	0.0872	0.396
0.006	0.1361	0.302	0.1076	0.396	0.0940	0.399
0.008	0.1506	0.329	0.1200	0.409	0.1059	0.402
0.01	0.1629	0.350	0.1307	0.418	0.1162	0.405
0.02	0.2076	0.413	0.1703	0.443	0.1549	0.411
0.03	0.2381	0.445	0.1980	0.455	0.1823	0.413
0.04	0.2614	0.466	0.2197	0.463	0.2038	0.414
0.05	0.2803	0.480	0.2374	0.468	0.2215	0.414
0.06	0.2962	0.491	0.2524	0.471	0.2365	0.414
0.08	0.3219	0.506	0.2769	0.476	0.2609	0.414
0.1	0.3418	0.517	0.2961	0.479	0.2802	0.415
0.2	0.3990	0.543	0.3521	0.487	0.3367	0.415
0.3	0.4245	0.552	0.3774	0.489	0.3624	0.415
0.4	0.4388	0.555	0.3914	0.490	0.3766	0.415
0.5	0.4486	0.556	0.4007	0.491	0.3860	0.415
0.6	0.4564	0.557	0.4080	0.491	0.3932	0.415
0.8	0.4693	0.558	0.4198	0.491	0.4049	0.415
1	0.4803	0.558	0.4297	0.491	0.4147	0.415
2	0.5205	0.559	0.4661	0.491	0.4507	0.415
3	0.5487	0.559	0.4918	0.492	0.4761	0.415
4	0.5708	0.559	0.5118	0.492	0.4959	0.415
5	0.5889	0.559	0.5283	0.492	0.5122	0.415

**Figure Captions**

Fig 1. A schematic of a rectangular passage with coordinates.

Fig 2d. The effects of frictional heating on the wall-bulk temperature difference for different  $MDa$  values in the absence of wall heat flux, when (a)  $b/a = 10$ , (b)  $b/a = 2$ , (c)  $b/a = 4$ , (d)  $b/a = 10$ .

Fig 3-a.  $Nu_D$  versus  $(x/a)/Pe$  for different  $Br$  and aspect ratio values, (a) when  $MDa=0.001$  and (b) when  $MDa=1$ .

Fig 4-a. Fully developed  $Nu_D$  versus  $Br$ ,  $MDa$ , and aspect ratio values, (a) when  $b/a=1$  and (b) when  $b/a=10$ .

Figure 5. Variation of  $Ns$  versus  $Br$  for different values of  $MDa$ .

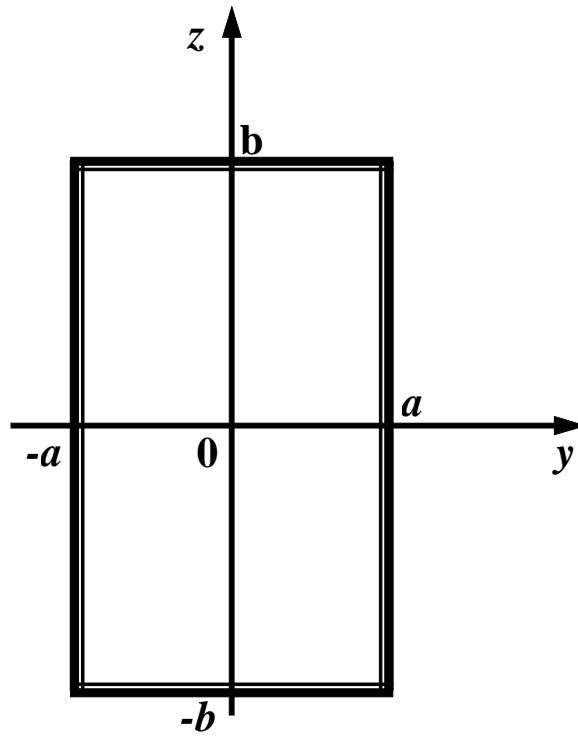
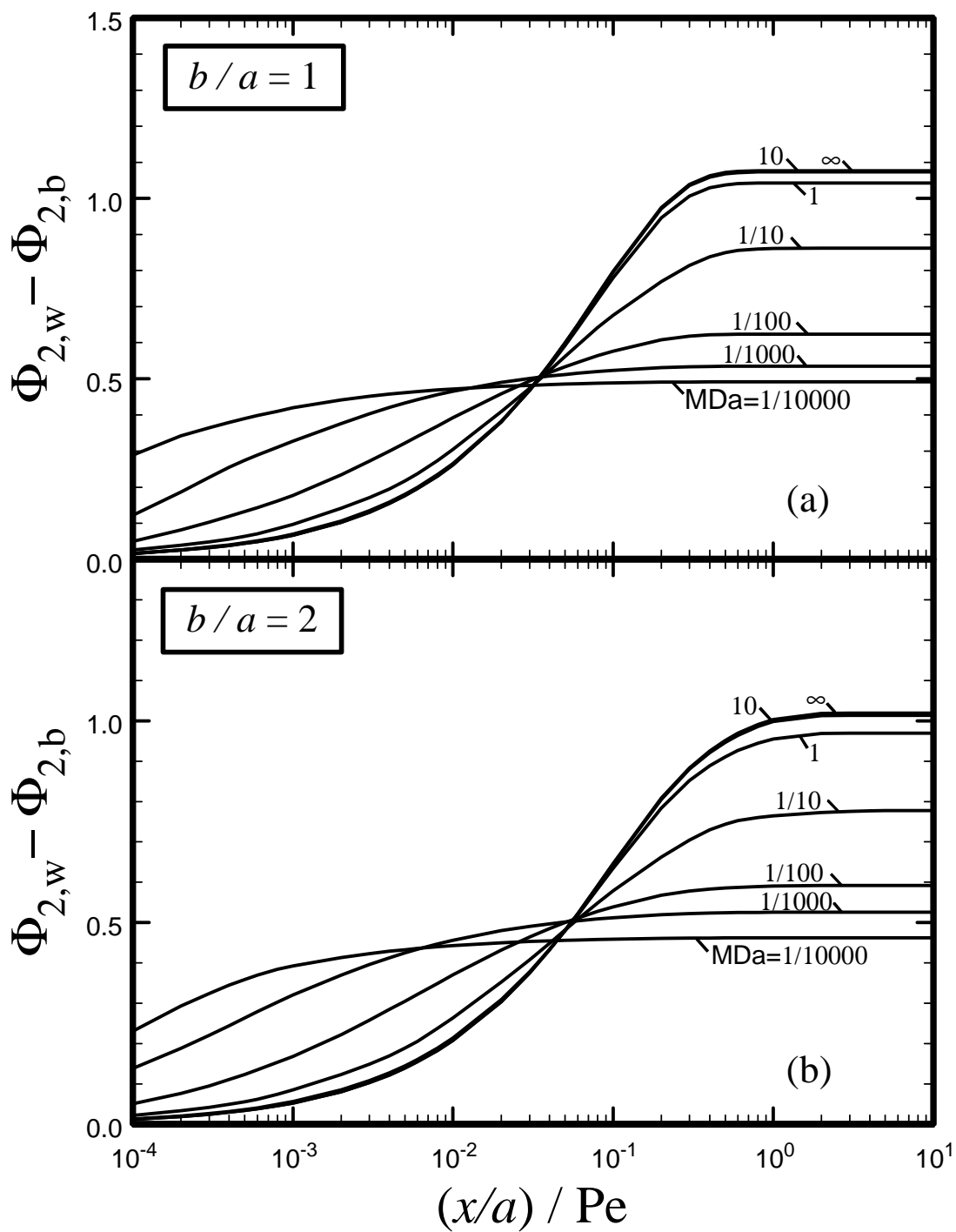


Fig 1. A schematic of a rectangular passage with coordinates.



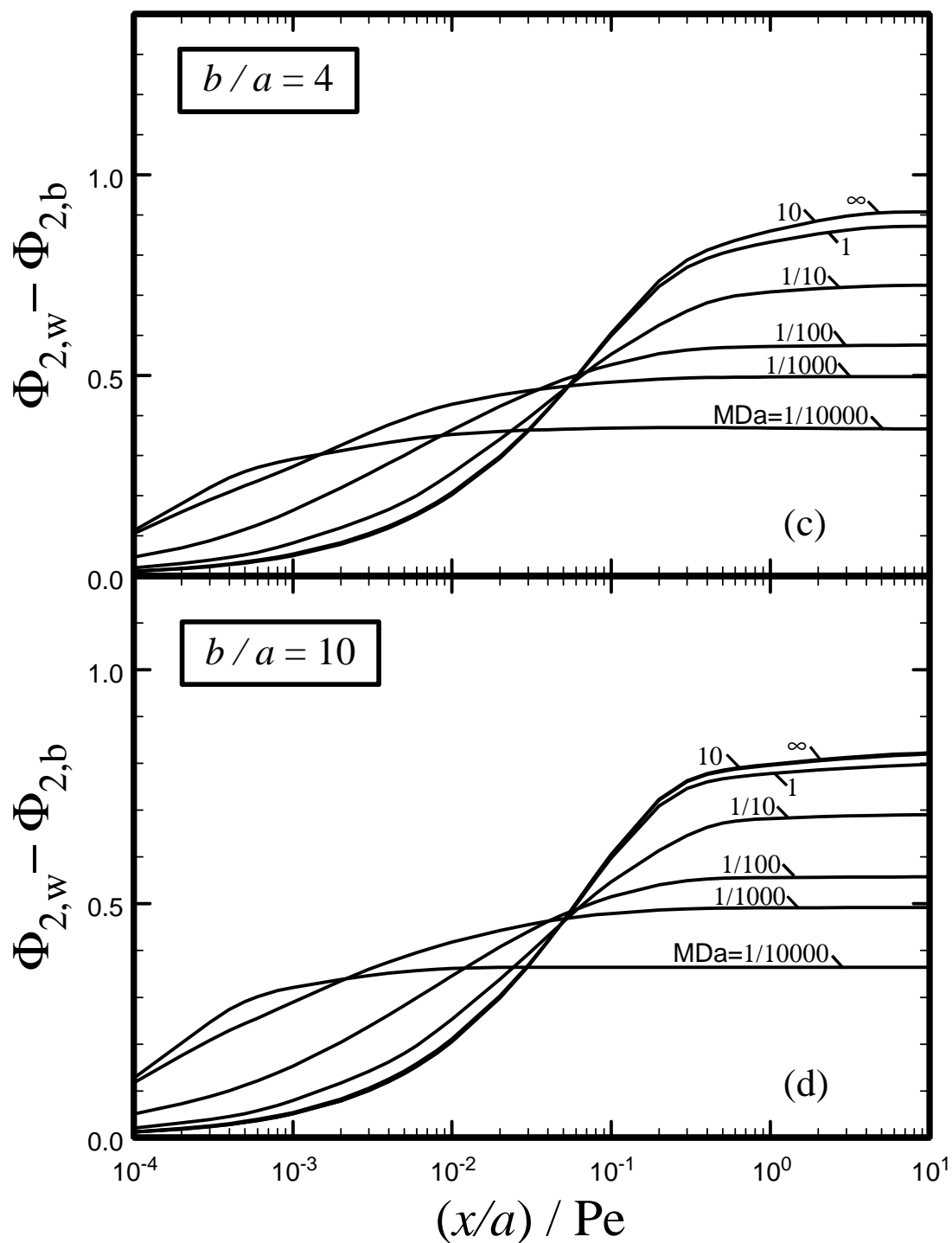


Fig 2. The effects of frictional heating on the wall-bulk temperature difference for different  $MDa$  values in the absence of wall heat flux, when (a)  $b/a = 10$ , (b)  $b/a = 2$ , (c)  $b/a = 4$ , (d)  $b/a = 10$ .



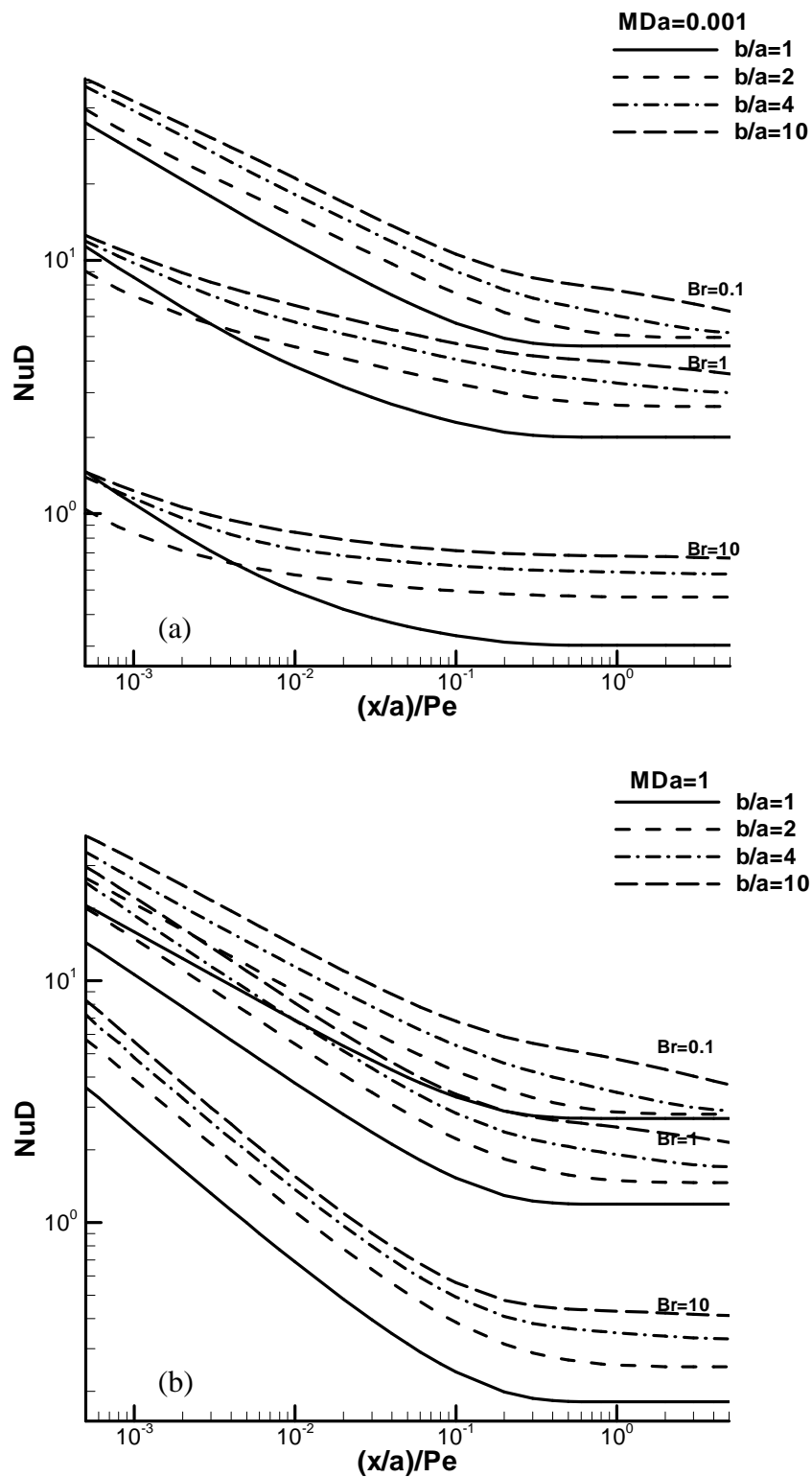


Fig 3.  $Nu_D$  versus  $(x/a)/Pe$  for different  $Br$  and aspect ratio values, (a) when  $MDa=0.001$  and (b) when  $MDa=1$ .

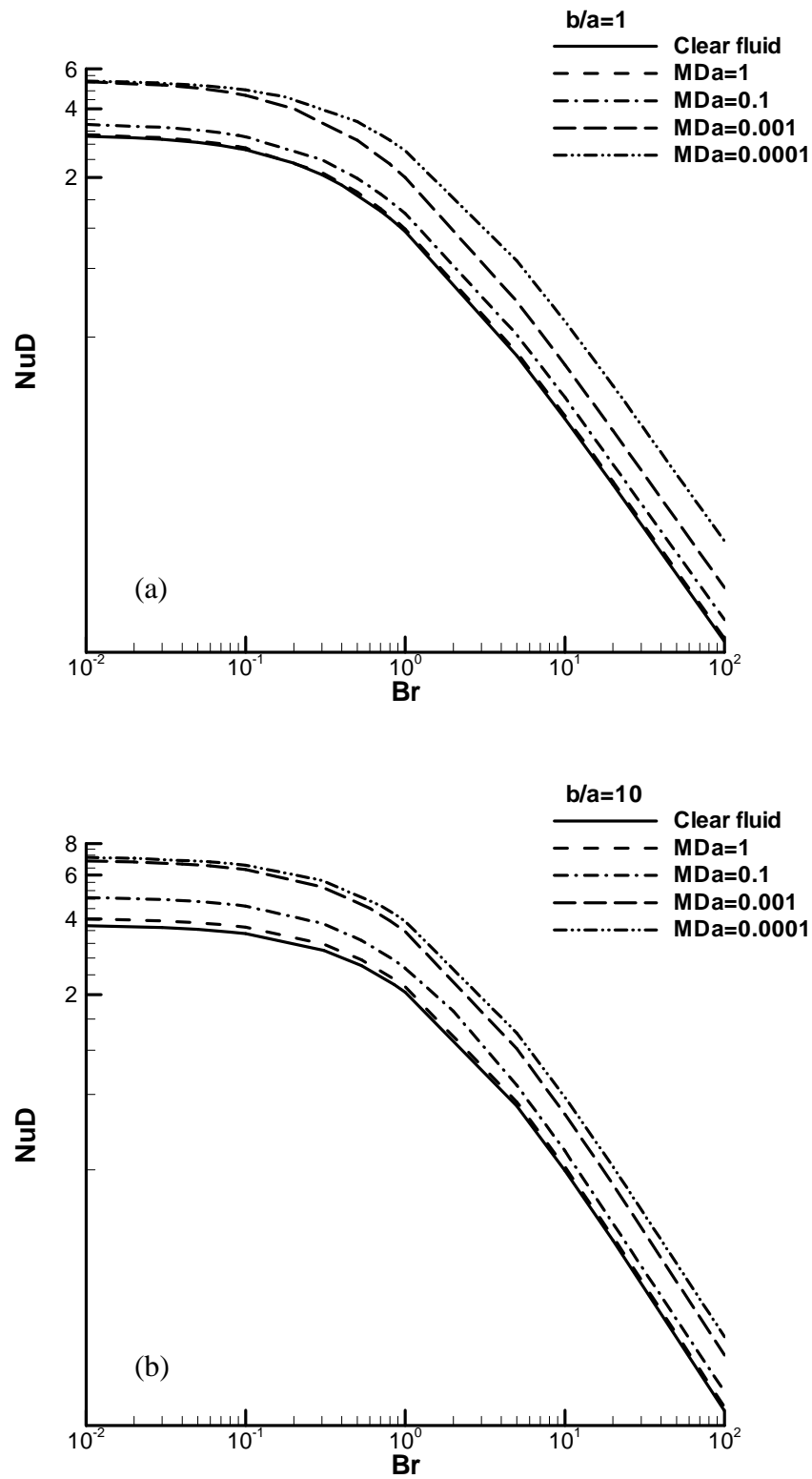


Fig 4. Fully developed  $Nu_D$  versus  $Br$ ,  $MDa$ , and aspect ratio values, (a) when  $b/a=1$  and (b) when  $b/a=10$ .

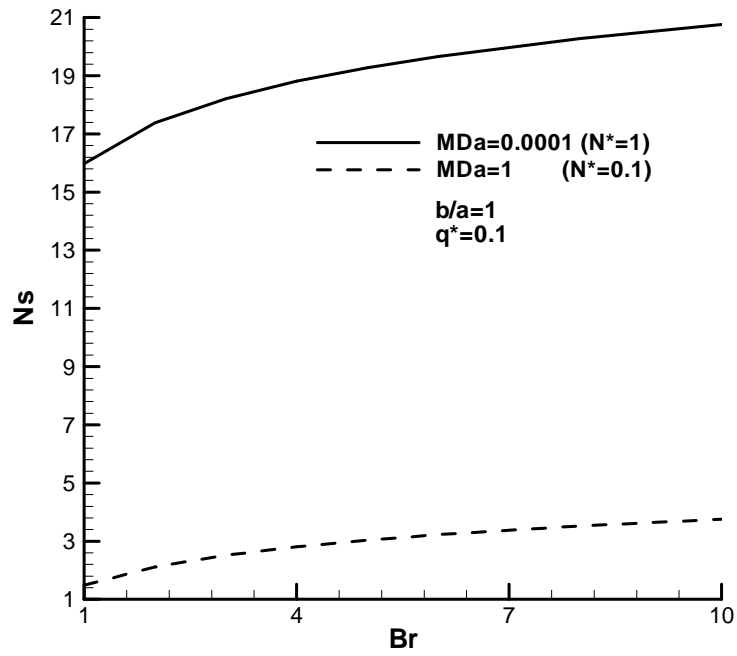


Fig 5. Variation of  $N_s$  versus  $Br$  for different values of  $MDa$ .